NANOSYSTEMS: PHYSICS, CHEMISTRY, MATHEMATICS, 2013, 4 (3), P. 370–377

PREPARATION AND ANTIMICROBIAL OBSERVATIONS OF ZINC DOPED NANOHYDROXYAPATITE

C. Deepa[1], A. Nishara Begum[2]* and S. Aravindan[3]

[1]Department of Physics, Vellalar College for Women (Autonomous), Erode-12
[2]Department of Physics, Chikkaiah Naicker College, Erode-4, Phone: +919443544946
[3]Department of Physics, Government Arts College (Autonomous), Salem-7
*anishara@yahoo.com

PACS 87.85.jc; 87.83.+a; 82.33.Ln; 61.46.Df; 68.37.Hk

Hydroxyapatite [$Ca_{10}(PO_4)_6(OH)_2$, HAp] is the major constituents of bones and hard tissues in mammals. In the last few years, HAp nanoparticles have been used as an ideal tool for the transformation of human hard tissues due to their high biocompatibility and easy biodegradability. Currently, metals are widely used in orthopedics to increase the bioactivity of hydroxyapatite. Among these metals, zinc is an essential trace element present in human bones and teeth. It plays important roles in increasing osteoblast adhesion and alkaline phosphatase activity of bone cells. In the present study, different amounts of pure and ZnO (0% – 43%) doped nano Hydroxyapatite powders were synthesized by the sol-gel method. The properties of pure and Zn doped nHAp powders were characterized using X-ray diffraction (XRD), Scanning electron microscopy (SEM), and Energy dispersive X-ray analysis (EDAX). The results of X-ray diffraction studies revealed the progressive increase in the average crystallite size from 49 to 100 nm with increasing ZnO concentration found to be 49–100 nm. The in vitro antimicrobial activities of the synthesized pure and Zn-doped nHAp powders were investigated against gram-negative bacterial strains using the disc diffusion method. The antimicrobial activities of pure and doped nHAp samples were observed irrespective of the ZnO content.

Keywords: Nano hydroxyapatite, Zinc oxide, Antimicrobial.

1. Introduction

Recently, the development of hydroxyapatite [$Ca_{10}(PO_4)_6(OH)_2$, HAp] with various additives has been one of the primary aims in the field of biomaterials, mainly to obtain superior quality materials suitable for use in artificial bone substitution. It is well known that, hydroxyapatite has a chemical similarity to the inorganic portion of human bone. The emerging trend of bone tissue engineering with hydroxyapatite has attracted intense interest due to its biofunctional properties, such as bioactivity and biocompatibility. Hap's properties such as morphology, stoichiometry, crystallinity and crystal size distribution (CSD) have great influence in the production of materials for biomedical applications. Hence, it is essential to optimize how these HAp properties are affected by different additives. Obviously, the incorporation of foreign elements can drastically alter the properties of HAp. It has already been demonstrated that introducing CO_3^{2-} and SiO_4^{4+} ions into the crystal lattice of HAp is effective at improving its degradation rate [1]. Since, the degradation rate of HAp plays a vital role in determining its biological performance, the inclusion of additives and their quantities attracts more significance.

Biological apatite is basically an impure form of Hap, but the non-stoichiometric HAp which incorporates a variety of trace ions such as Ca^{2+}, Mg^{2+}, Sr^{2+}, Ba^{2+}, Pb^{2+}, Zn^{2+}, Cu^{2+}, Na^{+}, K^{+}, Fe^{3+}, etc. is also useful to prepare the HAp with an atomic ratio (trace ion/P) of 1.5 – 1.67 [1], which is an essential requirement for it to become a biological apatite. The biological performance of HAp has been found to be improved with the incorporation of trace metal ions

such as zinc, silver and manganese, which exhibit their vibrant role in improving the biological ability of HAp during the additions [2]. Among the metal ions, zinc is one that is abundantly present as a trace element in bone minerals [3], in addition, zinc promotes the bone density and prevents bone loss [4].

The synthesis of nano biomaterials with a specific range of particle sizes, morphologies and chemical compositions has always been a challenge for researchers. In recent years, interest in the development of zinc oxide (ZnO) nano particles has been greatly increased, mainly because of their altered physical, chemical and biological properties. The development of nano HAp is more significant because of its specific affinity towards many adhesive proteins and its influence on bone cell differentiation and mineralization process. In orthopedics, post-surgical infections on implant materials is a major issue. The role of zinc like coatings on implant material is well documented to minimize bacterial adhesion. It is hoped that the incorporation of ZnO nanoparticles with a biomineral such as HAp can provide useful outcomes towards the development of anti-microbial requirements. In general, the anti-microbial activity of the zinc ion is involved in three major processes, e.g. protein deactivation, microbial membrane interaction and thereby structural change and permeability.

Recently, nano-sized particles have gained importance in biomedical fields, since the reduced size and surface activated particles are able to exhibit entirely new behaviors during dissolution and precipitation. Earlier reports [5] reveal the successful incorporation of metal ions with HAp, but they failed to demonstrate antimicrobial effects. The aim of this research is to synthesize zinc oxide doped nano-HAp powders and to examine their crystallinity, *in vitro* and plot antimicrobial activity against zinc oxide content.

2. Materials and Methods

Pure nano-HAp powders were prepared employing the sol-gel method with 0.55 M of calcium hydroxide $Ca(OH)_2$ (95% SIGMA ALDRICH) and 0.33 M of di ammonium hydrogen phosphate $(NH_4)_2{\cdot}HPO_4$ (99% SIGMA ALDRICH) respectively, used as sources for calcium and phosphorous. $Ca(OH)_2$ and $(NH_4)_2HPO_4$ were dissolved in 500 ml de-ionized water separately to obtain a stoichiometric molar ratio of 1.67. The pH of each aqueous solution was maintained at $\sim$11 by the addition of ammonium hydroxide solution NH_4OH (99%, SIGMA ALDRICH) [6]. A gelatinous white precipitate was produced by the dropwise addition of $(NH_4)_2HPO_4$ solution to the vigorously stirred $Ca(OH)_2$ solution at 333 K for an hour. Then, the precipitate was aged for 24 h at room temperature followed by washing three times with de-ionized water and dried in hot air oven at 423 K for 10 h. The dried powder was then milled using a mortar and pestle and finally calcined in an alumina crucible using a muffle furnace at 673 K for 5 h.

Nano-HAp samples with varying amounts of zinc oxide were synthesized using mixed aqueous solutions of prepared pure nano-HAp powder and zinc oxide. The dopants were used in the amount of 0, 10, 25, 50 and 75 wt. % (hereafter named as (a) Z_0H, (b) $Z_{10}H$, (c) $Z_{25}H$, (d) $Z_{50}H$ and (e) $Z_{75}H$). The mixed solutions were stirred for an hour. The obtained suspensions were filtered and dried in a hot air oven at 373 K for 5 h. The resultant pure and ZnO doped nano-HAp powders were characterized by XRD and SEM-EDAX.

2.1. X-ray Diffraction (XRD)

X-ray diffraction (XRD) studies were used to observe the structural properties of prepared pure and zinc oxide-doped nano-HAp powders. The analyses were carried out using a PAN analytical X'PERT-PRO diffractometer with high intensity of CuKα (wavelength $\lambda = 1.54060$ Å) radiation. The diffraction spectra were recorded in the angle 2θ ranging from

10° to 90°. The average crystallite size of pure and ZnO doped HAp nano powders were calculated using the Debye-Scherrer's formula [7]

$$D = 0.9\lambda/\beta\cos\theta, \tag{1}$$

where D is the crystallite size in nanometers, λ is the wavelength of CuKα radiation (1.5406 Å), β is full width of the peak at half of the maximum (FWHM) and θ is the diffraction angle of the corresponding reflection. The unit cell volume (V) and lattice parameters a and c of pure and ZnO incorporated HAp nano powders are calculated using the equations (2 & 3).

$$V = 2.589a^2c, \tag{2}$$

$$1/d_{hkl}^2 = 4/3\left[h^2 + hk + k^2\right]/a^2 + l^2/c^2, \tag{3}$$

where d is the crystallite size, h, k and l are miller indices of the plane, a and c are lattice constants.

2.2. Fourier Transform Infrared Spectroscopy (FTIR)

Fourier transform Infrared (FTIR) spectroscopy (PERKIN ELMAR; SPECTRUM RX1) was used to identify the elemental composition of pure and ZnO doped HAp nano powders. The FTIR spectra were obtained over the region from 400–4000 cm^{-1} in pellet form for 1 mg powder samples mixed with 200 mg spectroscopic grade KBr.

2.3. Morphology and Elemental Analysis (SEM/EDAX)

The Scanning Electron Microscopy (SEM) was performed using a JEOL JSM 6390, SEI model to determine microstructure and particle size on the surface of nano-HAp powders. The elemental analyses on the surface of pure and doped nano-HAp powders were performed by Energy dispersive X-ray analysis.

2.4. Antimicrobial Activity

The antibacterial activity of the prepared nano-HAp samples was tested against the bacterial strain *Klebsiella pneumonia* (ATCC 13883) by the modified disc-diffusion method [8]. The bacterial species were cultured for 24 h at 310 K and thereafter, the growth inhibition zones around the disc were measured.

3. Results and Discussion

3.1. XRD Characterization

Figure 1 shows the XRD patterns of the pure and ZnO incorporated HAp samples. The observed diffraction peaks of all prepared samples ensured the emergence of calcium rich phosphate apatite phases by matching well with the peaks in the standard JCPDS data file (09-0432). The intensity of the diffraction peak of plane (211) of HAp increased with the ZnO content, mainly because of the preferential orientation of ZnO in the apatite crystal. The peak intensity of the ZnO-incorporated HAp peak, increased with increasing ZnO content. Therefore, the added zinc content was also involved in the formation of HAp. The measured crystallite size, lattice parameter values and unit cell volumes are shown in Table 1. These data confirm the emergence of apatite mineral on the nanometer scale. The measured average crystallite size and unit cell volume of the HAp increased with increasing ZnO content. Particularly, the cell parameter a gradually increased with ZnO while another parameter c fluctuated with the incorporation of ZnO above 25 wt%. According to Fuzeng Ren et al. [7], the lattice parameters

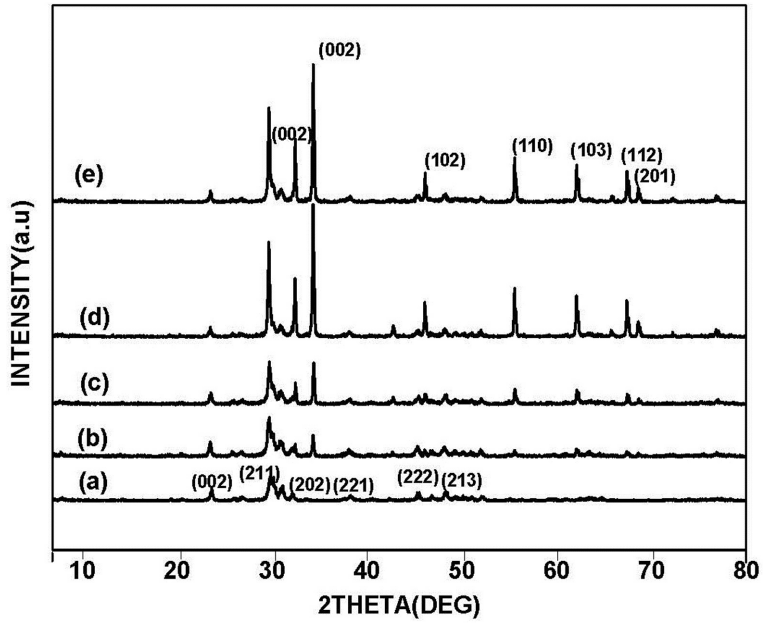

FIG. 1. XRD pattern of pure and Zn added HAp Samples
(a – Z_0H, b – $Z_{10}H$, c – $Z_{25}H$, d – $Z_{50}H$, e – $Z_{75}H$)

TABLE 1. Structural parameters of the zinc free and added HAp crystalline samples

Sample code	Average Crystallite Size D (nm)	Cell parameters		Unit cell volume V (Å)^3
		a (Å)	c (Å)	
Z_0H	49	9.4226	6.833	525
$Z_{10}H$	77	9.4225	6.8666	527
$Z_{25}H$	82	9.4395	6.8536	528
$Z_{50}H$	86	9.4561	6.8692	531
$Z_{75}H$	99	9.4901	6.864	535

a and c of crystalline HAp increased with the incorporation of ZnO. In addition, the substitution of H_2O in the lattice for OH sites in ZnO-doped HAp resulted in the increase of lattice parameter values [9].

3.2. Fourier Transforms Infrared Spectroscopy (FTIR) Analysis

The FTIR spectra of pure and ZnO-doped HAp nano powders synthesized by the sol-gel method are shown in Fig. 2. The FT-IR bands observed at 962 and 472 cm^{-1} were assigned to symmetric stretching modes ν_1 and ν_2 of phosphate group. Peaks observed at 568 and 603 cm^{-1} were assigned to ν_4 O-P-O bending bands corresponding to nano HAp. The ν_3 P-O asymmetric stretching mode was observed from 1041–1091 cm^{-1}. The bands observed at 3569 and 634 cm^{-1} were due to the stretching vibration of hydroxyl groups. The peak observed at 1430 cm^{-1} is a residue of atmospheric carbon dioxide present during the synthetic process. The bands at 3430 and 1637 cm^{-1} in HAp were attributed to the presence of lattice water. Bands observed at 1430 and 1637 cm^{-1} decreased with increasing ZnO content. According to FT-IR results, there is no obvious peak present for any other impurity [10].

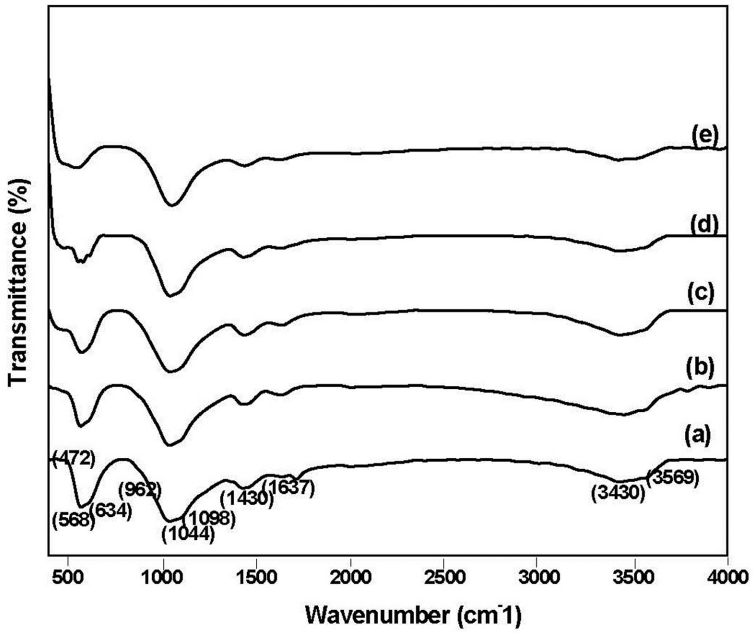

FIG. 2. FTIR spectra of pure and ZnO doped HAp nano powders (a – Z_0H, b – $Z_{10}H$, c – $Z_{25}H$, d – $Z_{50}H$, e – $Z_{75}H$)

3.3. SEM-EDAX Analysis

The morphologies and elemental analyses of pure and ZnO-doped nano-HAp samples were examined employing scanning electron microscopy (SEM) and energy dispersive X-ray (EDAX) analysis as shown in Fig. 3. The SEM micrographs revealed the emergence of rod-like crystalline species in ZnO-doped samples. The micrograph confirmed that particle sizes ranged from 49–67 nm with the incorporation of ZnO [10]. The result of elemental analysis (EDAX) of pure and ZnO-doped nano HAp confirmed the presence of Ca, P, O and Zn. The observed elemental concentration confirmed the Ca-P rich apatite crystalline phase. As expected, the elemental concentration of Zn was found to increase with increased ZnO content in HAp. The resultant Ca/P ratio of pure HAp was observed as 1.45, while in ZnO-incorporated samples, it increased up to the addition of 25 wt. % and decreases with further additions of ZnO to 75 wt. %.

3.4. Antimicrobial Activity

In vitro antibacterial activity of the synthesized pure and ZnO-incorporated nanoHAp samples were examined against Gram-negative *Klebsiella Pneumoniae* bacteria. Irrespective of the ZnO content, all the prepared HAp samples exhibited antimicrobial activity. The resultant data are shown in Table 2. These data revealed the influence ZnO had in decreasing the antimicrobial activity of the HAp as shown in Fig. 4. At 200 μg /ml, the sample Z_0H recorded the highest level of antimicrobial activity against *Klebsilla pneumoniae* by exhibiting the highest inhibition zone diameter. The zone diameter decreased with increased ZnO content, as shown in Fig. 5. It is obvious that the antibacterial property of apatite samples was dependent on the molecular structure of compound, the types of bacterial strains and the solvent used [11]. The incorporation of ZnO resulted in the formation of nano HAp with a modified structure and reduced antimicrobial activity.

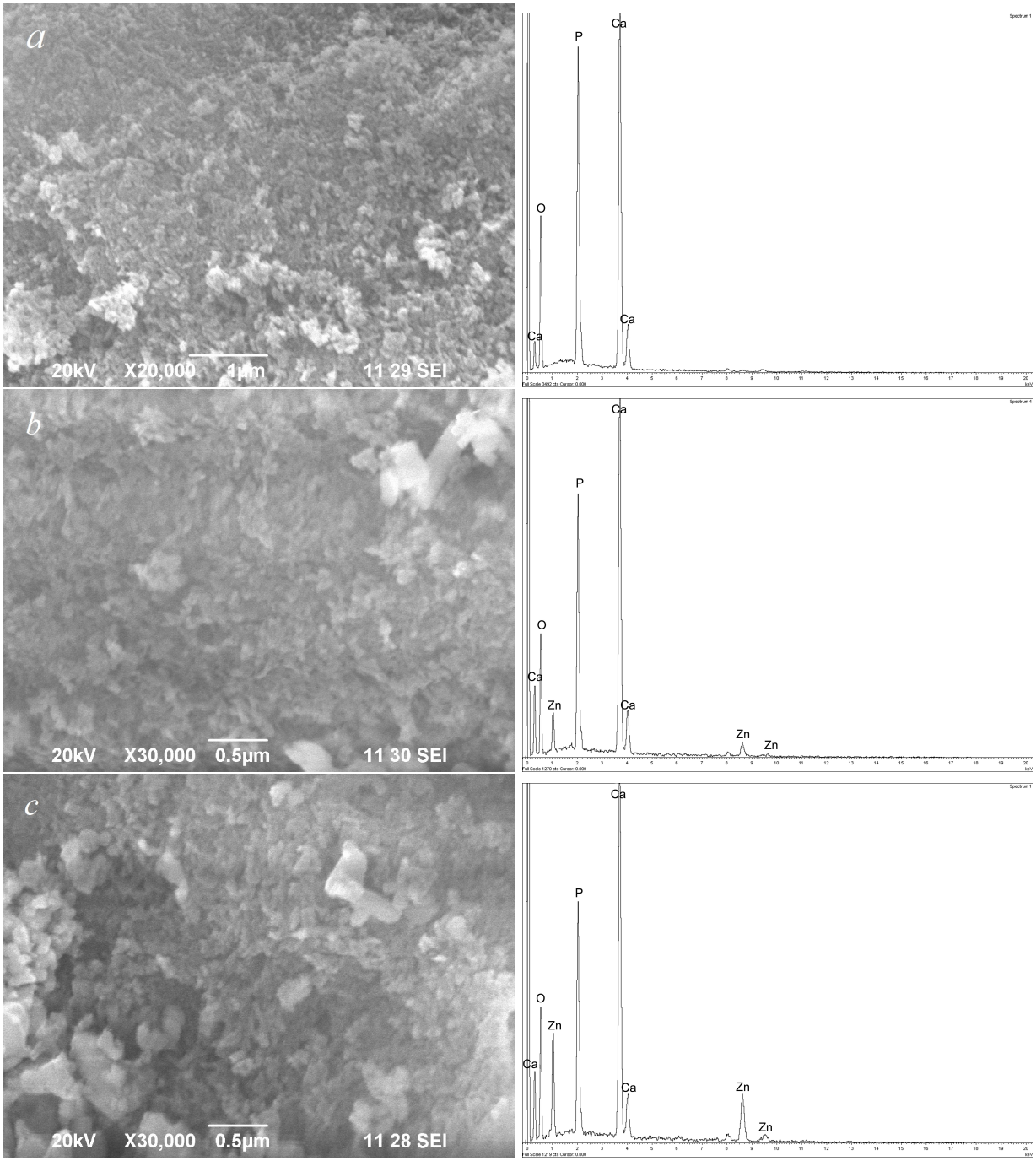

See the figure's caption on the next page

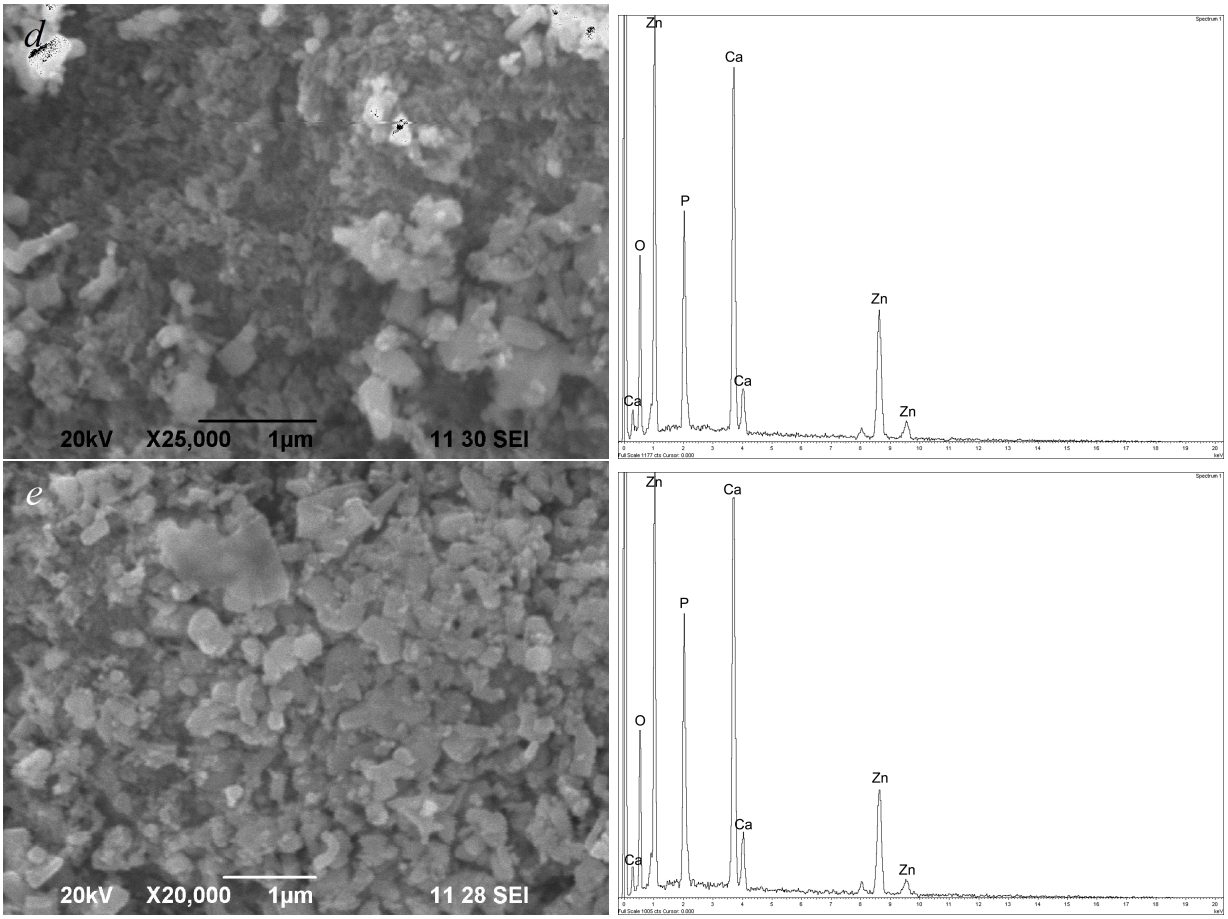

FIG. 3. SEM and EDAX images of Zinc free and added HAp samples (a – Z_0H, b – $Z_{10}H$, c – $Z_{25}H$, d – $Z_{50}H$, e – $Z_{75}H$)

TABLE 2. Antibacterial activity of pure and ZnO added nano HAp

Organism	Sample name (representation of Zone of inhibition (diameter in mm))				
Klebsiella pneumonia	Z_0H	$Z_{10}H$	$Z_{25}H$	$Z_{50}H$	$Z_{75}H$
	200 μg/ml	200 μg/ml	200 μg/ml	200 μg/ml	200 μg/ml
	15	14	12	12	11

4. Conclusions

Pure and ZnO-incorporated nano HAp samples were prepared employing the sol-gel method. The obtained XRD results confirmed the crystallite size of the samples in nanoscale. The influence of ZnO was used to increase the average crystallite size and unit cell volume of the Ca-P apatite crystal. The ZnO incorporations modified the morphology of HAp in rod like structure. Elemental analyses confirmed the emergence of calcium rich apatite crystalline phases. The *in vitro* antimicrobial activity of HAp was shown to be decreased by the addition of zinc oxide.

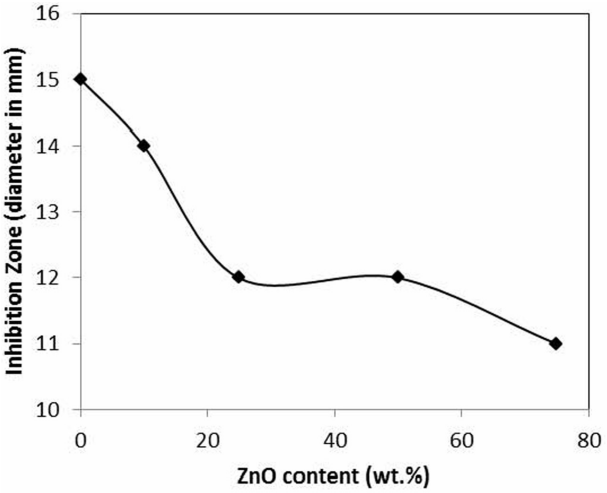

FIG. 4. Antimicrobial activity of HAp against ZnO additions

a – Z_0H b – $Z_{10}H$ c – $Z_{25}H$ d – $Z_{50}H$ e – $Z_{75}H$

FIG. 5. Antibacterial activity of Pure and ZnO-HAp against *Klepsilla pneumonia*

References

[1] D.G. Guo, Y. Wang, K. Han, W. Xu. Characterization, physico-chemical properties and biocompatibility of La-incorporated apatites. *Acta Biomaterialia*, **5**, P. 3512–3523 (2009).

[2] G. Mestres, C. Le Van, M.-P. Ginebra. Silicon-Stabilized α-tricalcium phosphate and its use in a calcium phosphate cement: Characterization and cell response. *Acta Biomaterialia*, **8**, P. 1169–1179 (2012).

[3] A. Ito, M. Otsuka, et al. Zinc-containing tricalcium phosphate and related materials for promoting bone formation. *Curr Appl phys*, **5**, P. 402-6 (2005).

[4] R.Z. Legeros. Calcium phosphate-based materials containing Zinc, Magnesium, Fluoride and carbonate. US Patent 7, 419,680. September 2 (2008).

[5] T.N. Kim, Q.L. Feng, et al. Antimicrobial effects of metal ions (Ag^{+}, Cu^{2+}, Zn^{2+}) in hydroxyapatite. *J. Mater. Sci. Mater. Med.*, **9**, P. 129–134 (1998).

[6] T.K. Anee, M. Ashok, M. Palinichamy, S. Narayana Kalkura. A novel technique to synthesize hydroxyapatite at low temperature. *Materials Chemistry and Physics*, **80**, P. 725–730 (2003).

[7] F. Ren, R. Xin, X. Ge, Y. Leng. Characterization and structural analysis of zinc-substituted hydroxyapatites. *Acta Biomaterialia*, **5**, P. 3141–3149 (2009).

[8] A.W. Baur, W.M.M. Kirby, J.C. Scherris, M. Turck. Antibiotic susceptibility testing by a standardized single disk method. *Amer. J. Cl. Pathol*, **45**, P. 493–496 (1966).

[9] F. Miyaji, Y. Kono, Y. Suyama. Formation and structure of zinc-substituted calcium hydroxyapatite. *Mater. Res. Bull*, **40**, P. 209–220 (2005).

[10] M.H. Santos, Luiz Guilherme, Dias Heneine. Synthesis and Characterization of calcium phosphate/collagen biocomposites doped with Zn^{2+}. *Material Science and Engineering C*, **28**, P. 563–571 (2008).

[11] A. Tripathi, S. Saravanan, S. Pattnaik. Bio composite scaffolds containing chitosan/nano-hydroxyapatite/nano-copper-zinc for bone tissue engineering. *International Journal of Biological Macromolecules*, **50**, P. 294–299 (2012).